HHS Public Access

Author manuscript

*Neuron*. Author manuscript; available in PMC 2017 January 06.

Published in final edited form as:

*Neuron*. 2016 January 6; 89(1): 100–112. doi:10.1016/j.neuron.2015.11.030.

# Role of Tet1/3 Genes and Chromatin Remodeling Genes in Cerebellar Circuit Formation

**Xiaodong Zhu**[1], **David Girardo**[2], **Eve-Ellen Govek**[1], **Keisha John**[1], **Marian Mellén**[3], **Pablo Tamayo**[2], **Jill P. Mesirov**[2], and **Mary E Hatten**[1,*]

[1]Laboratory of Developmental Neurobiology, The Rockefeller University, New York, NY 10065

[2]Broad Institute of MIT and Harvard, Cambridge, MA 02142

[3]Laboratory of Molecular Biology, The Rockefeller University, New York, NY 10065

## Summary

Although mechanisms underlying early steps in cerebellar development are known, evidence is lacking on genetic and epigenetic changes during the establishment of the synaptic circuitry. Using metagene analysis, we report pivotal changes in multiple reactomes of epigenetic pathway genes in cerebellar granule cells (GCs) during circuit formation. During this stage, Tet genes are up-regulated and vitamin C activation of Tet enzymes increases the levels of 5-hydroxymethylcytosine (5hmC) at exon start sites of up-regulated genes, notably axon guidance genes and ion channel genes. Knockdown of *Tet1* and *Tet3* by RNA interference in *ex vivo* cerebellar slice cultures inhibits dendritic arborization of developing GCs, a critical step in circuit formation. These findings demonstrate a role for Tet genes and chromatin remodeling genes in the formation of cerebellar circuitry.

## Introduction

The cerebellar cortex is a key model for cortical histogenesis as it consists of only two principle neurons, the granule cell (GC) and Purkinje cell (PC), and as the development and physiology of the cerebellar circuitry are well established (Ito, 1984; Palay SL, 1974; Sillitoe and Joyner, 2007) (Figure S1A). While classical studies have revealed critical roles

*Corresponding Author: hatten@rockefeller.edu.

**Accession Numbers**: The GEO database accession number for the TRAP microarray data and 5hmC-enriched DNA sequencing data reported in this paper is GSE74402.

Supplemental Information: Supplemental Information includes supplemental experimental procedures, seven figures and four tables, and can be found with this article online.

**Author Contributions:** Drs. Mary E. Hatten, Xiaodong Zhu, Eve-Ellen Govek and Keisha John designed all experiments. Dr. Xiaodong Zhu carried out TRAP RNA purification, for ES cell experiments, and 5hmC analyses. Dr. Keisha John carried out TRAP RNA purification from native GCs. Dr. Eve-Ellen Govek carried out Tet1/3 RNA interference assays. Dr. Marian Mellén helped to perform 5hmC pull-down and library preparation. David Girardo, Drs. Pablo Tamayo and Jill Mesirov designed and carried out the computational analysis of gene expression data. Drs. Mary E. Hatten, Xiaodong Zhu, Eve-Ellen Govek, Pablo Tamayo and Jill Mesirov wrote the manuscript.

for morphogens (Alder et al., 1999; Chi et al., 2003; Lee and Jessell, 1999; McMahon and Bradley, 1990) and transcription factors (TFs) (Ben-Arie et al., 1997; Liu et al., 1999; Sillitoe and Joyner, 2007; Wang and Zoghbi, 2001) in establishing the cerebellar territory and specifying cerebellar neurons during development, evidence is lacking on the genetic and epigenetic mechanisms that control formation of the cerebellar circuitry.

The translating ribosome affinity purification (TRAP) method (Doyle et al., 2008; Heiman et al., 2008), which profiles mRNAs in specific cell types that are transcriptionally active, provides a powerful approach for analyzing global gene expression patterns in CNS neurons. In addition to revealing genome-wide features of the transcriptome of identified CNS cell types, this approach has also offered insight into epigenetic regulatory mechanisms. The critical importance of epigenetic, chromatin remodeling through processes that include histone modifications and DNA methylation and demethylation is underscored by recent studies showing a linkage between disruption of these processes and human disease, including cancers of the CNS (Robertson, 2005; Wang et al., 2007a). Epigenetic modifications to DNA, especially 5-methylcytosine (5mC) by DNA methyltransferases has been studied extensively (Smith and Meissner, 2013). The recent discovery that 5mC can be converted to 5hmC by the ten-eleven translocation (Tet) family of dioxygenases (Ito et al., 2010; Tahiliani et al., 2009) and that 5hmC is relatively abundant in mammalian brain (Kriaucionis and Heintz, 2009; Szulwach et al., 2011; Tahiliani et al., 2009) as well as that 5hmC distribution correlates with cell-type specific gene expression in CNS neurons (Mellen et al., 2012), suggests that the Tet-mediated generation of 5hmC has an important role in the epigenetic control of CNS neuronal differentiation.

In the present study, we used TRAP methodology to analyze global gene expression patterns, including the expression of genes involved in epigenetic regulatory pathways of developing cerebellar GCs. To assess the similarities and differences between global transcription profiles over a series of developmental stages and to compare them with differentiated ES cells, we used a metagene projection methodology (Brunet et al., 2004; Tamayo et al., 2007). This approach allows us to find the most salient patterns of gene expression over time and identify the corresponding key biological features in an unbiased manner. Using this methodology, we show that there are pivotal changes in a broad range of chromatin remodeling genes during the developmental stage when the cerebellar circuitry forms. To analyze DNA cytosine modification in developing GCs, we quantitated genome-wide 5hmC distribution. To test the function of Tet genes in cerebellar GC development, we then used an ES cell model and functional assays in developing cerebellar cortex. Activation of Tet enzymes in GCs treated with vitamin C resulted in elevated 5hmC levels at exon start sites of up-regulated genes, notably axon guidance genes and ion channel genes; knockdown of *Tet1* and *Tet3* resulted in a failure of granule cell dendritic arborization, which is a critical step in circuit formation. These studies suggest a role for Tet genes and chromatin remodeling genes during the formation of CNS synaptic circuitry.

## Results

### Profiling Granule Cell Gene Expression Using TRAP Methodology and Metagene Analysis

To provide a comparative analysis of genome-wide gene expression at key developmental stages, we used TRAP methodology (Doyle et al., 2008; Heiman et al., 2008), which combines CNS cell type-specific transgene expression of affinity-tagged enhanced GFP (EGFP) fused to the large ribosomal subunit protein L10a to purify ribosomes and the mRNAs they are translating. As NeuroD1 is a specific marker for postmitotic GCs, we purified mRNA from postmitotic GCs from *Tg(NeuroD1-Egfp-L10a)* mouse cerebellar tissue at P0, when NeuroD1+ GCs begin to exit the cell cycle; at P7, the peak of GC glial-guided migration from the external granule cell layer (EGL) to the internal granule cell layer (IGL); at P12-P21, the period when the cerebellar circuitry forms (Hansel et al., 2001; Kalinovsky et al., 2011; Sotelo, 2004) and coordinated motor behavior develops (Ito, 1972); and at P56, when the cerebellum is mature in the adult mouse (Figure 1A, B).

To generate a time series model of gene expression for developing cerebellar GCs, we used metagene projection to identify the most salient features of transcriptional behavior of cerebellar GCs at key developmental stages. This was done by factoring the matrix of Affymetrix microarray profiles of GC samples (genes by time points) (Figure S1B-D) into the product of two matrices, (genes by metagenes) times (metagenes by time points), which approximates the input data array (Brunet et al., 2004; Tamayo et al., 2007). Biological annotations for each metagene were derived by first projecting the original expression data set into a space of pathways and biological processes from the Molecular Signatures Database (MSigDB, www.broadinstitute.org/gsea/msigdb) (Subramanian et al., 2005), using a single sample version of Gene Set Enrichment Analysis (Barbie et al., 2009) and finding those that are most similar to the metagene's profile (See Supplemental Experimental Procedures). For additional annotation, we formed a set of the genes that most highly contribute to each metagene (i.e., with highest values in the corresponding column of the first matrix) and computed the significance of their overlap with gene sets in curated databases such as MSigDB and DAVID (Huang da et al., 2009). Seven metagenes (C1_7-C7_7, Figure 1C) were identified. Metagene 7 was of special interest, because it revealed genes that were up regulated during the time when the cerebellar circuitry forms (P12-P21).

### Temporal Regulation of Epigenetic Pathway Genes during the Formation of Cerebellar Circuitry

Pivotal changes occurred in reactomes for the major classes of epigenetic pathway genes, represented in multiple metagenes, during the period of circuit formation (Figure 1D). These reactomes included genes that encode proteins that regulate chromatin remodeling (Figure 2A, S2A), histone modification (Figure 2B-D, S2B), and DNA methylation and demethylation (Figure 1D, S2C) (Robertson, 2005; Wang et al., 2007a, b). Especially dramatic, was the discovery of serial changes in groups representing ATP-dependent chromatin remodeling genes, histone methylation and acetylation genes, and DNA methylation and demethylation genes, including the Tet genes, which generate 5hmC epigenetic marks (Ito et al., 2010; Tahiliani et al., 2009) (Figure 1D, S2D). The expression of genes related to DNA methylation (DNA methyltransferases) and histone

acetyltransferases (HATs) peaked first, preceding that of Tet enzymes and histone deacetylases (HDACs) (Figure 1D, 2A-D, S2D). We examined these in more detail (see below). During the same time window, axon guidance genes and ion channel genes, as well as genes that are required for axon and dendrite outgrowth and synapse formation, were also up-regulated (Figure 1E, S3).

Among chromatin remodeling reactomes, pivotal changes occurred in the expression levels of ATP-dependent chromatin remodeling complexes, genes that function in the balance between proliferation and differentiation (de la Serna et al., 2006) when GCs undergo terminal differentiation, and centromere proteins (Figure 2A). Among these were *Smarc* genes, which belong to the SWI/SNF and ISWI family (Wang et al., 2007b) and *Cenp* genes, which assemble on centromeric DNA to epigenetically control chromosome segregation during mitosis (Westhorpe and Straight, 2013). All of these genes were down regulated after P12, when post-migratory GCs form connections with ingrowing afferent axons. These findings are consistent with recent studies showing an important role for *Smarca5* (*Snf2h*) in the early development of the cerebellum (Alvarez-Saavedra et al., 2014), where a conditional ablation of *Smarca5* affected PC dendritic arborization during cerebellar development, and with the finding that a conditional loss of *Smarca4* or *Smarcb1* in GCs impairs neurogenesis and cerebellar development, resulting in mice with severe ataxia (Moreno et al., 2014).

Among histone methyltransferases (HMTs), the levels of a number of genes increased after neurogenesis, while others decreased in postmitotic cells (Figure 2D). Importantly, HMTs that increased when the circuitry forms (P12 onward), mediate the formation of epigenetic marks that activate gene expression. Among these were HMTs that generate H3K4me1, 2 or 3, including *Setd1a*, *Setd7*, *Smyd3*, *Mll1*, *Mll2*, *Mll3* and *Mll5*. At this developmental stage, the level of most of the genes that mediate formation of repressive epigenetic marks went down. These included *Ezh2*, the HMT responsible for the formation of H3K27me3, as well as *Setdb1*, *Setdb2*, *Suv39h1*, *Suv39h2*, which generate H3K9me3, and *Suv420h1* and *Suv420h2*, which generate H4K20me3. The changes in gene levels were confirmed by qRT-PCR analysis (Figure 2E-H, S2E) and the histone modifications in developing cerebella were examined by immunohistochemistry (Figure S4A).

## Increase in Tet Gene Expression and 5hmC Levels During the Period of Circuit Formation in Developing GCs

We focused on the Tet genes because of studies showing 10-fold higher levels of 5hmC in brain than in other tissues (Kriaucionis and Heintz, 2009; Szulwach et al., 2011; Tahiliani et al., 2009), because of evidence that the distribution of 5hmC differs among CNS cell types (Mellen et al., 2012) and that these differences suggest a possible role in neuronal differentiation and/or synaptic function. Our gene expression assays, as well as qRT-PCR measurements, on cerebellar GCs revealed up-regulation of all three Tet genes in GCs between P12 and P21 (Figure 3A), with higher levels of *Tet1* and *Tet3* and lower levels of *Tet2* (Figure 3B-C). As recent studies demonstrate that vitamin C activates Tet enzymes and induces Tet-dependent DNA demethylation (Blaschke et al., 2013; Yin et al., 2013), we also analyzed the expression of vitamin C transporters in developing GCs. The levels of vitamin

C transporters *Slc2a1*, *Slc2a3*, *Slc23a1* and *Slc23a2* in developing GCs peaked at P18 (Figure 3A), after which levels remained fairly constant. These findings were confirmed by qRT-PCR measurements (Figure 3D). Thus the levels of both Tet genes and vitamin C transporter genes increase in post-migratory GCs.

We then examined the localization of 5hmC during cerebellar development. By liquid chromatography/mass spectrometry (LC-MS) (Figure 3E), 5hmC levels were lowest at P0 and P7, the peak of GC neurogenesis, increasing dramatically between P12 and P18, when the cerebellar circuitry forms. 5hmC levels rose further at P56, when the circuitry is mature. A small increase in 5mC levels occurred over these stages of cerebellar development, with higher levels seen at P56. Similar results were seen with dot-blot analysis, which revealed a three-fold increase in cerebellar 5hmC levels over development (Figure S4B-C). By immunocytochemistry, highly proliferating GC progenitors (GCPs) in the EGL of P0-P7 mouse cerebellar cortex had undetectable levels of 5hmC, with much higher levels in NeuroD1-EGFP-positive, post-migratory, differentiated GCs in the IGL where there was broad double labeling with antibodies against 5hmC and GFP (Figure S4D). In contrast, staining for 5mC was high in proliferating GCPs in the EGL (prior to *NeuroD1* expression), postmitotic NeuroD1-EGFP-positive GCs migrating across the molecular layer (ML) and differentiated GCs in the IGL (Figure S4E). These findings extend previous studies on 5hmC during cortical development (Lister et al., 2013) by demonstrating a dramatic increase in 5hmC levels during the stage when the circuitry forms in the developing cerebellar cortex.

## Treatment of ES Cell-derived GCs with Vitamin C Up-regulates the Expression of Axon Guidance/Dendrite Outgrowth and Ion Channel Genes

To analyze the function of Tet genes and changes in 5hmC marks in GC development, we used two approaches. First, we used a stem cell model of GCs, inducing GC differentiation by treating embryonic stem (ES) cells generated from *Tg(NeuroD1-Egfp-L10a)* transgenic mice with factors that induce GC differentiation *in vivo* (Salero and Hatten, 2007) to assay changes in gene expression after Tet enzyme activation. Prior experiments on ES cells lacking *Tet1* and *Tet2* demonstrated that vitamin C treatment selectively activates Tet enzymes (Blaschke et al., 2013; Yin et al., 2013). After vitamin C treatment, the percentage of NeuroD1-EGFP+ ES cell-derived GCs in the culture increased two fold, suggesting that vitamin C promoted the differentiation of ES cells into GCs (Figure S5A-B). Gene expression assays using TRAP methodology showed dramatic increases in the expression of axon guidance genes (Figure 4A). This was the case for most of the genes in the axon guidance reactome, including axon guidance ligands and receptors, much like the concurrent up-regulation of the Tet gene cluster and the axon guidance gene cluster between P12-P21 in endogenous GCs (Figure 4B-C, 1D-E, S3). In addition, the level of expression of all of the 19 genes encoding ion channels and synaptic proteins that we assayed by qRT-PCR, increased after vitamin C treatment (Figure 4D, S5C-E). Similar results were obtained for native P7 GCs treated with vitamin C (data not shown). The relative level of 5hmC increased approximately five fold in vitamin C-treated ES cell-derived GCs compared with control, untreated cells (Figure 4E-F). No significant change in the relative level of 5mC occurred after vitamin C treatment. These findings demonstrate that vitamin C activation of Tet enzymes, which increased levels of 5hmC, result in up-regulation of genes involved in

axon guidance, as well as ion channel genes involved in neuronal conductance and activity. Importantly a large number of studies demonstrate that axon guidance genes, including many of those found in our analyses, also function in dendrite outgrowth (Clifford et al., 2014; Polleux et al., 2000; Whitford et al., 2002), thus playing critical roles in the establishment of neuronal circuitry.

## Increased Expression Levels of Axon Guidance and Ion Channel Genes Correlate with Higher Levels of 5hmC at Exon Start Sites

To examine changes in 5hmC distribution and levels of expression of genes in regions with 5hmC marks, we labeled 5hmC with a selective labeling strategy known as hMe-Seal (Mellen et al., 2012; Song et al., 2011), purified 5hmC-enriched genomic DNA fragments and carried out DNA deep sequencing (Table S3). Genome-wide analysis of 5hmC distribution in both native cerebellar GCs and ES cell-derived GCs showed that 5hmC marks were present in exons, and secondary in introns and other regulatory elements (Figure 5A, S6, S7B). Taken together with our microarray results and analyses, these experiments further indicate that the highest levels of 5hmC map to the exon start sites of genes with the highest expression levels (Figure 5B). Across all axon guidance genes, 5hmC levels increased an average of 1.7 fold in ES cell-derived GCs upon vitamin C treatment (Figure S7A, C). Elevated levels of 5hmC signal mapped to many axon guidance genes that also function in dendrite extension during circuit formation, including *Sema5a*, *Sema6a*, *Plxna2*, *Slit2* and *Robo1*, as well as ion channel genes, such as *Scn8a* (Figure 5C-H). Thus, increased 5hmC levels correlated with up regulation of axon guidance/dendrite formation genes and of ion channel genes (Figure 4B-D, S7C). These findings suggest that 5hmC levels regulate gene expression, and that in GCs, 5hmC regulates the expression of genes involved in axon/dendrite formation and of ion channel/synaptic genes during the formation of the cerebellar circuitry.

## Tet RNAi Knockdown Decreases 5hmC Levels and Down-regulates the Expression of Axon Guidance and Ion Channel Genes in Cerebellar GCs

To determine whether Tet enzymes regulate 5hmC levels in native cerebellar GCs, we purified GCs from mouse cerebellum at P7, transfected them with equal amounts of *Tet1* and *Tet3* shRNA plasmids that co-expressed the fluorophore Venus, or a control scrambled shRNA that co-expressed Venus (Figure 6A). After 3DIV, qRT-PCR assays revealed a 69% reduction in *Tet1* mRNA and a 71% reduction in *Tet3* mRNA; no change in cell viability occurred (Figure 6B-C). By dot blot analysis, 5hmC levels decreased dramatically in transfected GCs, while 5mC levels increased slightly (Figure 6D). In control experiments, 5hmC levels in NeuroD1-Egfp-L10a ES cells increased dramatically after treatment with vitamin C; no change in 5hmC levels was observed in Tet1/Tet3 double knockdown NeuroD1-Egfp-L10a ES cells treated with vitamin C (Figure S7D-E). We then used qRT-PCR to determine whether the level of expression of axon guidance and ion channel genes, which were up-regulated by vitamin C treatment, decreased after Tet RNAi knockdown. Those experiments showed a large decrease in the expression levels of axon guidance and ion channel genes (Figure 6E). These experiments suggest that *Tet1* and *Tet3* increase 5hmC levels in GCs and specifically up-regulate the expression of selected axon guidance and ion channel genes that are important for GC development.

### Knockdown of Tet1 and Tet3 Impairs GC Dendritic Arborization

To test the function of Tet genes in GC development, we used RNAi methodology to knock down *Tet1* and *Tet3* in cerebellar GCs in brain slices. P7-P8 cerebella were electroporated with equal amounts of *Tet1* and *Tet3* shRNA plasmids that co-express the fluorophore Venus to visualize the cells. *Tet1* and *Tet3* knockdown dramatically impaired dendritic arborization of post-migratory GCs in the IGL (Figure 7A-B). While approximately 75-80% of control cells electroporated with scrambled shRNA extended multiple dendritic processes in the IGL, only 10-15% of GCs electroporated with *Tet1* and *Tet3* shRNAs did so (Figure 7C). Instead, the majority of *Tet1* and *Tet3* deficient GCs extended a single process, similar to the leading process of migrating GCs. Interestingly, Tet knockdown did not impair earlier developmental steps, including parallel fiber outgrowth or glial-guided migration of postmitotic GCs from the EGL into the IGL (Figure 7D). These findings suggest that *Tet1* and *Tet3* are required for dendritic arborization, a critical step in the formation of cerebellar circuitry, in post-migratory GCs during cerebellar development.

## Discussion

The present study demonstrates pivotal changes in multiple chromatin remodeling reactomes in cerebellar neurons during the developmental stage when the cerebellar circuitry forms. Using a combination of TRAP methodology and metagene analysis, we found a previously unreported temporal regulation of multiple classes of chromatin remodeling genes after immature neurons migrate into the neuronal layer where they form synaptic connections with ingrowing afferent axons. We found that among chromatin remodeling genes, expression of Tet genes, which generate 5hmC epigenetic marks, showed a sharp increase in levels during this stage of GC development. Significantly, genome-wide analysis of 5hmC distribution in both native GCs and ES cell-derived GCs showed that 5hmC marks were highest at the exon start sites of the most highly expressed genes. Importantly, treatment of ES cell-derived GCs with vitamin C, which activates Tet enzymes, up regulated 5hmC levels and expression of axon guidance and ion channel genes, and higher 5hmC levels were tightly correlated with increased expression of axon guidance/dendrite outgrowth genes and many ion channel genes. Furthermore, functional assays in developing mouse cerebellum showed that *Tet1/3* knockdown by RNA interference severely impaired dendritic arborization, a critical step in circuit formation in post-migratory GCs. Taken together, these findings suggest that vitamin C activates Tet enzymes to generate 5hmC epigenetic marks at exon start sites, leading to the increased expression of genes critical to circuit formation and function during GC development.

Importantly, the rise in levels of Tet gene expression and 5hmC marks in post-migratory GCs in the developing cerebellum persists through adulthood. The recent discovery that 5hmC is present in the mammalian genome and that it is particularly enriched in neurons (Kriaucionis and Heintz, 2009; Szulwach et al., 2011; Tahiliani et al., 2009) has stimulated a great deal of interest in its role in differentiation and the stabilization of neuronal phenotypes. Indeed, 5hmC is approximately 10-fold more abundant in neurons than in some peripheral tissues or ES cells (Kriaucionis and Heintz, 2009; Szulwach et al., 2011), and recent studies show differences in 5hmC distribution among brain regions, including the

hippocampus, cerebellum and frontal cortex (Lister et al., 2013; Szulwach et al., 2011), with 5hmC preferentially abundant in genes with synapse-related functions in both human and mouse brain (Khare et al., 2012). Heintz and colleagues further demonstrated the critical contribution of 5hmC accumulation within actively expressed gene bodies to cell-specific gene expression and CNS neuron function (Mellen et al., 2012). Our findings significantly extend previous bulk measurements of 5hmC during postnatal cortical development (Lister et al., 2013) by showing an increase in 5hmC in an identified cerebellar neuron during the formation of the cerebellar circuitry. Our studies also extend the studies of Mellen et al., who showed that 5hmC maps to gene bodies of genes in adult cerebellar neurons (Mellen et al., 2012), by providing developmental data and showing that 5hmC maps to the start sites of exons of genes with up-regulated expression after activation of Tet enzymes. Moreover, our findings show that increased 5hmC levels correlate with up-regulated expression of axon guidance and ion channel genes during the developmental stages when cerebellar neurons integrate into the neuronal layer where they form synaptic connections with ingrowing afferent axons. These findings suggest that 5hmC levels regulate gene expression, and that in GCs, 5hmC regulates the expression of genes involved in axon/dendrite formation and of ion channel/synaptic genes during the formation of the cerebellar circuitry.

The present study also highlights the critical role of Tet enzymes in the generation of 5hmC in developing neurons. Since the demonstration that Tet enzymes oxidize 5mC to 5hmC in mammalian cells (Guo et al., 2011; Ito et al., 2010; Tahiliani et al., 2009), several studies have shown that Tet enzymes are important transcriptional regulators in neuronal development, including *Xenopus* eye development (Xu et al., 2012) and olfactory system development (Colquitt et al., 2013). Our studies strongly support the conclusion that vitamin C activates Tet generation of 5hmC in CNS neurons, since treatment of ES cell-derived GCs with vitamin C increased 5hmC levels by 5 fold and up regulated axon guidance genes and ion channel protein genes. Importantly, the present study also shows a tight coupling between the increase in vitamin C transporter genes and Tet gene levels in developing GCs. Both vitamin C transporter genes and Tet gene levels rise in the second postnatal week, after neurogenesis and migration are complete. Given the role of vitamin C as an agonist of Tet dioxygenases, it will be interesting to investigate whether vitamin C transporters are required for 5hmC generation and function in CNS neurons.

Our finding that *Tet1/3* knockdown by RNA interference impaired dendrite formation in developing GCs in an *ex vivo* system is the first demonstration of a functional role for Tet genes in terminal steps of GC differentiation. These findings are consistent with other recent studies showing that *Tet3* gene overexpression disrupts axon targeting in the developing olfactory system (Colquitt et al., 2013) and that *Tet1* has important functions in memory formation (Kaas et al., 2013) and neuronal activity-related gene expression in memory extinction (Rudenko et al., 2013). In addition, a large number of studies demonstrate that axon guidance genes, including many of those found in our analyses, also function in dendrite outgrowth (Clifford et al., 2014; Polleux et al., 2000; Whitford et al., 2002), thus playing critical roles in the establishment of neuronal circuitry. Taken together, these studies underscore the importance of Tet genes to CNS circuit formation and function.

The present findings extend the classical paradigm for CNS development in which morphogens and TFs establish the rostrocaudal axis of the CNS and specify different classes of neurons within emerging brain regions. Our findings underscore the importance of chromatin remodeling to CNS neuronal development and the critical role of Tet-5hmC signaling in circuit formation during brain development. Metagene analysis identified salient changes in gene expression during cerebellar development and revealed a previously unreported temporal regulation of multiple classes of chromatin remodeling genes after immature neurons migrate into the neuronal layer where they form synaptic connections with ingrowing afferent axons. Among chromatin remodeling genes, Tet genes function in the generation of 5hmC, which regulates the expression of axon guidance/dendrite formation genes and ion channel genes that underlie the development of the cerebellar circuitry. Our finding that 5hmC maps to the exon start sites of the exons of highly expressed genes suggests that 5hmC levels regulate gene expression during this pivotal stage of cortical development. In the future, it will be important to examine the role of chromatin remodeling gene regulation in neuronal activity (Greer and Greenberg, 2008; Qiu and Ghosh, 2008; Wheeler et al., 2012). Understanding the role of epigenetic regulation in the emergence of CNS circuitry will be important for understanding behavior and developmental disorders such as autism (Gabel et al., 2015; Loke et al., 2015).

## Experimental Procedures

### Es Cell Differentiation

The NeuroD1-TRAP mouse ES cell lines were isolated from heterozygous *Tg(NeuroD1-Egfp-L10a)* TRAP mice (Doyle et al., 2008; Heiman et al., 2008) and maintained using standard conditions. We refined our previous mouse ES cell differentiation protocol and differentiated NeuroD1-TRAP mouse ES cells into cerebellar GCs (See Supplemental Experimental Procedures) (Salero and Hatten, 2007). All protocols involving animals were approved by the Rockefeller University Institutional Animal Care and Use Committee.

### Purification of mRNA from Mouse Cerebella and Differentiated Mouse ES Cells

TRAP RNA from translating polysomes was extracted from differentiated NeuroD1-TRAP mouse ES cells at differentiation day 15 with and without vitamin C treatment, or mouse cerebella at progressively developmental periods (*Tg(NeuroD1-Egfp-L10a)* mice at P0, P7, P12, P18, P21 and P56), as previously described (Heiman et al., 2008). Each cell population was assayed in triplicate. For each sample, 500 ng of TRAP RNA was used for the in vitro synthesis of the biotin-labeled cRNA which was hybridized to Affymetrix GeneChip Mouse Gene 1.0 ST Array according to the manufacturer's instructions (See Supplemental Experimental Procedures).

### Genomic DNA Purification, Enzymatic Digestion and Liquid Chromatography–Mass Spectrometry (LC-MS) Analysis

Genomic DNA was purified from mouse cerebellar cortex at different developmental stages (P0, P7, P12, P18, P21 and P56) using DNeasy Blood & Tissue Kit (Qiagen) following the manufacturer's instructions. The extracted genomic DNA was digested to individual nucleosides with DNA Degradase Plus (Zymo Research). Three 897bp DNA standards, each

homogenous for either unmodified C, 5mC, or 5hmC (Zymo Research), were used to generate a calibration curve. The 5-Methyl-2′-deoxycytidine (5mC, Cayman Chemical) and 5-(Hydroxymethyl)-2′-deoxycytidine (5hmC, Cayman Chemical), were used as the internal standard for the MS quantitation of 5mC and 5hmC, respectively. The digested DNA solutions were subjected to LC-MS (Agilent Technologies, Palo Alto, CA) analysis for detection of C, 5mC and 5hmC. The mass spectrometer was operated in the positive ion mode. The multiple reaction monitoring (MRM) mode was adopted: m/z 242.200→126.005 for 5mC, m/z 258.200→142.105 for 5hmC, and m/z 228.200→112.105 for C. The measured percentage of 5mC and 5hmC in each experimental sample was calculated from the MRM peak area divided by the combined peak areas for 5mC plus 5hmC plus C (total cytosine pool) (See Supplemental Experimental Procedures).

### Dot-blot Assay

Genomic DNA was isolated from ES cell-derived GCs with and without vitamin C treatment, purified GCs or cerebellar cortex. Purified DNA was denatured in 0.1M NaOH, neutralized with 1M $NH_4OAc$ on ice, and then serially diluted twofold. Denatured DNA samples were spotted on nitrocellulose membrane (PROTRAN, Schleicher&Schuell). The blotted membrane was dried at 80 °C for 5 min, then DNA was fixed to the membrane by Stratagene UV Stratalinker 1800. The blotted membrane was washed in 2× SSC buffer for 10 min, and then blocked with Odyssey buffer (Li-Cor) diluted 1:1 in PBS (Odyssey:PBS) overnight at 4°C. Mouse anti-5mC antibody (1:1,000, Eurogentec) or rabbit anti-5-hmC antibody (1:10,000, Active Motif) in Odyssey:PBS was added for 2 h at room temperature. The membrane was washed three times for 10 min in PBST, and then incubated with either HRP-conjugated sheep anti-mouse immunoglobulin-G (IgG) or HRP-conjugated sheep anti-rabbit IgG (GE Healthcare) secondary antibodies in Odyssey:PBS for 2 h at room temperature. The membrane was then washed three times for 10 min in PBST and visualized by chemiluminescence with GE ECL (See Supplemental Experimental Procedures).

### 5hmC Pull-Down, Library Preparation and DNA Sequencing

Sorted cells (ES cell-derived GCs (GFP+), with and without vitamin C treatment) and purified GCs from P7 cerebella of *Tg(NeuroD1-Egfp-L10a)* mice, as described (Hatten, 1985), were manipulated in parallel during the procedure. Genomic DNA was purified from the above-mentioned cells. Sonicated DNA was end-repaired followed by ligation to adapters for HiSeq 2500 (Illumina Inc., San Diego, CA, USA) technology using TruSeq DNA HT Sample Prep Kit (Illumina) and following manufacturer's instructions. The 5hmC-enriched genomic DNA collection was performed as described (Mellen et al., 2012; Song et al., 2011). After purification, DNA was amplified as described in TruSeq DNA Sample preparation kit. The 5hmC-enriched DNA was then sequenced using Illumina platform obtaining more than $30\times10^6$, 50 bp single-end reads per sample (Table S3) (See Supplemental Experimental Procedures).

### *Ex Vivo* Cerebellar Electroporation, Organotypic Slice Culture and Imaging

shRNA oligos against mouse *Tet1* and *Tet3* were characterized previously (Guo et al., 2011; Ito et al., 2010) (Table S4) and the efficacy of shRNAs were further tested in cell culture

after electroporation. After P7-8 mouse cerebella were electroporated, coronal cerebellar slices were prepared and cultured for the times indicated in the figures. The fixed slices were incubated with primary antibodies, rabbit anti-GFP (Invitrogen) and mouse anti-Calbindin (Swant), washed and then incubated with Alexa Fluor conjugated-secondary antibodies for immunofluorescence (See Supplemental Experimental Procedures).

### Microarray Pre-processing and Non-negative Matrix Factorization

The Affymetrix microarray profiles of GC samples (Mouse Gene 1.0 ST Array) (Figure S1B-D) were processed using the *ExpressionFileCreator* tool in GenePattern to map gene probes into gene symbols (www.genepattern.org). The resulting expression dataset A, was decomposed using Non-negative Matrix Factorization into two matrices: $A \sim W \times H$, using the methodology from Brunet et al. 2004 and Tamayo et al. 2007, including a procedure to determine the number of metagenes.

### Metagene Gene Sets and Single-sample GSEA

For each metagene, a corresponding gene set was generated by considering the subset of genes with the highest amplitude (W matrix). These genes are chosen by sorting each column of W from largest to smallest, and then selecting only genes before the values reach a linear decay. These gene sets were then used to project the expression profile of the ES cell-derived GC samples into the same transcriptional landscape using single-sample GSEA (ssGSEA)(Barbie et al., 2009). For every metagene gene set and sample, ssGSEA provides estimates of the degree of enrichment for the metagene member genes. The metagene and gene set ssGSEA profiles were visualized using heat maps and multidimensional scaling biplot projections.

### Matching Pathways to Metagenes

To identify biological processes and pathways that were associated with the metagenes, we matched each metagene profile (row of H) against the samples' ssGSEA profiles corresponding to a large compendium of gene sets from the Molecular Signatures Database (MSigDB, www.broadinstitute.org/gsea/msigdb). To estimate the degree of association we used the Information Coefficient (IC).

### Analysis of 5hmC Data

The 5hmC data were analyzed following the methods as described (Song et al., 2011). The 5hmC filtered and unfiltered reads were mapped to the mm10 *mus musculus* genome using the program Bowtie2, and the 5hmC summits were calculated using Model-based Analysis of ChIP-Seq (MACS). To explore the enhancer region activity for each exon, the 5hmC summit landscape +/- 5000bp relative to exon start sites were considered. These summit landscapes, centered at the exon start site for each exon, were averaged together to obtain a condensed view for each gene. Similarly, the mean of the condensed 5hmC summit landscape for each gene in relevant gene sets were calculated and used to analyze concordant 5hmC across pathways. The 5hmC profiles for genes and gene sets were compared with metagene profiles described above, and between developmental types, to

verify epigenetic-expression correlations, and identify major epigenetic developmental changes.

## Supplementary Material

Refer to Web version on PubMed Central for supplementary material.

## Acknowledgments

We are grateful to Dr. Nathaniel Heintz for providing the *Tg(NeuroD1-Egfp-L10a)* TRAP line and for critical discussions on the manuscript. We also thank Drs. Cori Bargmann, Joseph Gleeson and Marc Tessier-Lavigne for critical comments on the manuscript and Dr. David Allis for reviewing the gene expression data. We thank Dr. Myriam Heiman for advice with the TRAP assays, David Murphy for qRT-PCR assays and Yin Fang for preparation of murine GCs. James Duffy prepared the line drawings in Figures 1B and S1A. The Rockefeller DNA Sequencing Core carried out the Affymetrix microarray and DNA sequencing, the Rockefeller University Flow Cytometry Resource Center carried out cell purifications and the Rockefeller Proteomics Resource Center carried out liquid chromatography–mass spectrometry analysis. We thank Connie Zhao, Svetlana Mazel, Henrik Molina and Joseph Fernandez from these Cores. Supported by funding from Le Fondation Sackler-The Sackler Foundation (MEH) and by grants NIH R01NS051778 (MEH), NIH R01CA154480 (JPM), NIH R01109467 (JPM), NIH R01GM074024 (JPM), NIH U54CA112962 (JPM) and NIH U54HG006093 (JPM).

## References

Alder J, Lee KJ, Jessell TM, Hatten ME. Generation of cerebellar granule neurons in vivo by transplantation of BMP-treated neural progenitor cells. Nature neuroscience. 1999; 2:535–540. [PubMed: 10448218]

Alvarez-Saavedra M, De Repentigny Y, Lagali PS, Raghu Ram EV, Yan K, Hashem E, Ivanochko D, Huh MS, Yang D, Mears AJ, et al. Snf2h-mediated chromatin organization and histone H1 dynamics govern cerebellar morphogenesis and neural maturation. Nature communications. 2014; 5:4181.

Barbie DA, Tamayo P, Boehm JS, Kim SY, Moody SE, Dunn IF, Schinzel AC, Sandy P, Meylan E, Scholl C, et al. Systematic RNA interference reveals that oncogenic KRAS-driven cancers require TBK1. Nature. 2009; 462:108–112. [PubMed: 19847166]

Ben-Arie N, Bellen HJ, Armstrong DL, McCall AE, Gordadze PR, Guo Q, Matzuk MM, Zoghbi HY. Math1 is essential for genesis of cerebellar granule neurons. Nature. 1997; 390:169–172. [PubMed: 9367153]

Blaschke K, Ebata KT, Karimi MM, Zepeda-Martinez JA, Goyal P, Mahapatra S, Tam A, Laird DJ, Hirst M, Rao A, et al. Vitamin C induces Tet-dependent DNA demethylation and a blastocyst-like state in ES cells. Nature. 2013; 500:222–226. [PubMed: 23812591]

Brunet JP, Tamayo P, Golub TR, Mesirov JP. Metagenes and molecular pattern discovery using matrix factorization. Proceedings of the National Academy of Sciences of the United States of America. 2004; 101:4164–4169. [PubMed: 15016911]

Chi CL, Martinez S, Wurst W, Martin GR. The isthmic organizer signal FGF8 is required for cell survival in the prospective midbrain and cerebellum. Development. 2003; 130:2633–2644. [PubMed: 12736208]

Clifford MA, Athar W, Leonard CE, Russo A, Sampognaro PJ, Van der Goes MS, Burton DA, Zhao X, Lalchandani RR, Sahin M, et al. EphA7 signaling guides cortical dendritic development and spine maturation. Proceedings of the National Academy of Sciences of the United States of America. 2014; 111:4994–4999. [PubMed: 24707048]

Colquitt BM, Allen WE, Barnea G, Lomvardas S. Alteration of genic 5-hydroxymethylcytosine patterning in olfactory neurons correlates with changes in gene expression and cell identity. Proceedings of the National Academy of Sciences of the United States of America. 2013; 110:14682–14687. [PubMed: 23969834]

de la Serna IL, Ohkawa Y, Imbalzano AN. Chromatin remodelling in mammalian differentiation: lessons from ATP-dependent remodellers. Nature reviews Genetics. 2006; 7:461–473.

Doyle JP, Dougherty JD, Heiman M, Schmidt EF, Stevens TR, Ma G, Bupp S, Shrestha P, Shah RD, Doughty ML, et al. Application of a translational profiling approach for the comparative analysis of CNS cell types. Cell. 2008; 135:749–762. [PubMed: 19013282]

Gabel HW, Kinde B, Stroud H, Gilbert CS, Harmin DA, Kastan NR, Hemberg M, Ebert DH, Greenberg ME. Disruption of DNA-methylation-dependent long gene repression in Rett syndrome. Nature. 2015; 522:89–93. [PubMed: 25762136]

Greer PL, Greenberg ME. From synapse to nucleus: calcium-dependent gene transcription in the control of synapse development and function. Neuron. 2008; 59:846–860. [PubMed: 18817726]

Guo JU, Su Y, Zhong C, Ming GL, Song H. Hydroxylation of 5-methylcytosine by TET1 promotes active DNA demethylation in the adult brain. Cell. 2011; 145:423–434. [PubMed: 21496894]

Hansel C, Linden DJ, D'Angelo E. Beyond parallel fiber LTD: the diversity of synaptic and non-synaptic plasticity in the cerebellum. Nature neuroscience. 2001; 4:467–475. [PubMed: 11319554]

Hatten ME. Neuronal regulation of astroglial morphology and proliferation in vitro. The Journal of cell biology. 1985; 100:384–396. [PubMed: 3881455]

Heiman M, Schaefer A, Gong S, Peterson JD, Day M, Ramsey KE, Suarez-Farinas M, Schwarz C, Stephan DA, Surmeier DJ, et al. A translational profiling approach for the molecular characterization of CNS cell types. Cell. 2008; 135:738–748. [PubMed: 19013281]

Huang da W, Sherman BT, Lempicki RA. Systematic and integrative analysis of large gene lists using DAVID bioinformatics resources. Nature protocols. 2009; 4:44–57. [PubMed: 19131956]

Ito M. Neural design of the cerebellar motor control system. Brain Res. 1972; 40:81–84. [PubMed: 4338265]

Ito, M. Cerebellum and Neural Control. New York: Raven Press; 1984.

Ito S, D'Alessio AC, Taranova OV, Hong K, Sowers LC, Zhang Y. Role of Tet proteins in 5mC to 5hmC conversion, ES-cell self-renewal and inner cell mass specification. Nature. 2010; 466:1129–1133. [PubMed: 20639862]

Kaas GA, Zhong C, Eason DE, Ross DL, Vachhani RV, Ming GL, King JR, Song H, Sweatt JD. TET1 controls CNS 5-methylcytosine hydroxylation, active DNA demethylation, gene transcription, and memory formation. Neuron. 2013; 79:1086–1093. [PubMed: 24050399]

Kalinovsky A, Boukhtouche F, Blazeski R, Bornmann C, Suzuki N, Mason CA, Scheiffele P. Development of axon-target specificity of ponto-cerebellar afferents. PLoS Biol. 2011; 9:e1001013. [PubMed: 21346800]

Khare T, Pai S, Koncevicius K, Pal M, Kriukiene E, Liutkeviciute Z, Irimia M, Jia P, Ptak C, Xia M, et al. 5-hmC in the brain is abundant in synaptic genes and shows differences at the exon-intron boundary. Nature structural & molecular biology. 2012; 19:1037–1043.

Kriaucionis S, Heintz N. The nuclear DNA base 5-hydroxymethylcytosine is present in Purkinje neurons and the brain. Science. 2009; 324:929–930. [PubMed: 19372393]

Lee KJ, Jessell TM. The specification of dorsal cell fates in the vertebrate central nervous system. Annual review of neuroscience. 1999; 22:261–294.

Lister R, Mukamel EA, Nery JR, Urich M, Puddifoot CA, Johnson ND, Lucero J, Huang Y, Dwork AJ, Schultz MD, et al. Global epigenomic reconfiguration during mammalian brain development. Science. 2013; 341:1237905. [PubMed: 23828890]

Liu A, Losos K, Joyner AL. FGF8 can activate Gbx2 and transform regions of the rostral mouse brain into a hindbrain fate. Development. 1999; 126:4827–4838. [PubMed: 10518499]

Loke YJ, Hannan AJ, Craig JM. The Role of Epigenetic Change in Autism Spectrum Disorders. Front Neurol. 2015; 6:107. [PubMed: 26074864]

McMahon AP, Bradley A. The Wnt-1 (int-1) proto-oncogene is required for development of a large region of the mouse brain. Cell. 1990; 62:1073–1085. [PubMed: 2205396]

Mellen M, Ayata P, Dewell S, Kriaucionis S, Heintz N. MeCP2 binds to 5hmC enriched within active genes and accessible chromatin in the nervous system. Cell. 2012; 151:1417–1430. [PubMed: 23260135]

Moreno N, Schmidt C, Ahlfeld J, Poschl J, Dittmar S, Pfister SM, Kool M, Kerl K, Schuller U. Loss of Smarc proteins impairs cerebellar development. The Journal of neuroscience : the official journal of the Society for Neuroscience. 2014; 34:13486–13491. [PubMed: 25274825]

Palay, SL. C.-P.V. Cerebellar cortex: cytology and organization. New York: Springer; 1974.

Polleux F, Morrow T, Ghosh A. Semaphorin 3A is a chemoattractant for cortical apical dendrites. Nature. 2000; 404:567–573. [PubMed: 10766232]

Qiu Z, Ghosh A. A calcium-dependent switch in a CREST-BRG1 complex regulates activity-dependent gene expression. Neuron. 2008; 60:775–787. [PubMed: 19081374]

Robertson KD. DNA methylation and human disease. Nature reviews Genetics. 2005; 6:597–610.

Rudenko A, Dawlaty MM, Seo J, Cheng AW, Meng J, Le T, Faull KF, Jaenisch R, Tsai LH. Tet1 is critical for neuronal activity-regulated gene expression and memory extinction. Neuron. 2013; 79:1109–1122. [PubMed: 24050401]

Salero E, Hatten ME. Differentiation of ES cells into cerebellar neurons. Proceedings of the National Academy of Sciences of the United States of America. 2007; 104:2997–3002. [PubMed: 17293457]

Sillitoe RV, Joyner AL. Morphology, molecular codes, and circuitry produce the three-dimensional complexity of the cerebellum. Annu Rev Cell Dev Biol. 2007; 23:549–577. [PubMed: 17506688]

Smith ZD, Meissner A. DNA methylation: roles in mammalian development. Nature reviews Genetics. 2013; 14:204–220.

Song CX, Szulwach KE, Fu Y, Dai Q, Yi C, Li X, Li Y, Chen CH, Zhang W, Jian X, et al. Selective chemical labeling reveals the genome-wide distribution of 5-hydroxymethylcytosine. Nature biotechnology. 2011; 29:68–72.

Sotelo C. Cellular and genetic regulation of the development of the cerebellar system. Prog Neurobiol. 2004; 72:295–339. [PubMed: 15157725]

Subramanian A, Tamayo P, Mootha VK, Mukherjee S, Ebert BL, Gillette MA, Paulovich A, Pomeroy SL, Golub TR, Lander ES, et al. Gene set enrichment analysis: a knowledge-based approach for interpreting genome-wide expression profiles. Proceedings of the National Academy of Sciences of the United States of America. 2005; 102:15545–15550. [PubMed: 16199517]

Szulwach KE, Li X, Li Y, Song CX, Wu H, Dai Q, Irier H, Upadhyay AK, Gearing M, Levey AI, et al. 5-hmC-mediated epigenetic dynamics during postnatal neurodevelopment and aging. Nature neuroscience. 2011; 14:1607–1616. [PubMed: 22037496]

Tahiliani M, Koh KP, Shen Y, Pastor WA, Bandukwala H, Brudno Y, Agarwal S, Iyer LM, Liu DR, Aravind L, et al. Conversion of 5-methylcytosine to 5-hydroxymethylcytosine in mammalian DNA by MLL partner TET1. Science. 2009; 324:930–935. [PubMed: 19372391]

Tamayo P, Scanfeld D, Ebert BL, Gillette MA, Roberts CW, Mesirov JP. Metagene projection for cross-platform, cross-species characterization of global transcriptional states. Proceedings of the National Academy of Sciences of the United States of America. 2007; 104:5959–5964. [PubMed: 17389406]

Wang GG, Allis CD, Chi P. Chromatin remodeling and cancer, Part I: Covalent histone modifications. Trends in molecular medicine. 2007a; 13:363–372. [PubMed: 17822958]

Wang GG, Allis CD, Chi P. Chromatin remodeling and cancer, Part II: ATP-dependent chromatin remodeling. Trends in molecular medicine. 2007b; 13:373–380. [PubMed: 17822959]

Wang VY, Zoghbi HY. Genetic regulation of cerebellar development. Nature reviews Neuroscience. 2001; 2:484–491. [PubMed: 11433373]

Westhorpe FG, Straight AF. Functions of the centromere and kinetochore in chromosome segregation. Current opinion in cell biology. 2013; 25:334–340. [PubMed: 23490282]

Wheeler DG, Groth RD, Ma H, Barrett CF, Owen SF, Safa P, Tsien RW. Ca(V)1 and Ca(V)2 channels engage distinct modes of Ca(2+) signaling to control CREB-dependent gene expression. Cell. 2012; 149:1112–1124. [PubMed: 22632974]

Whitford KL, Marillat V, Stein E, Goodman CS, Tessier-Lavigne M, Chedotal A, Ghosh A. Regulation of cortical dendrite development by Slit-Robo interactions. Neuron. 2002; 33:47–61. [PubMed: 11779479]

Xu Y, Xu C, Kato A, Tempel W, Abreu JG, Bian C, Hu Y, Hu D, Zhao B, Cerovina T, et al. Tet3 CXXC domain and dioxygenase activity cooperatively regulate key genes for Xenopus eye and neural development. Cell. 2012; 151:1200–1213. [PubMed: 23217707]

Yin R, Mao SQ, Zhao B, Chong Z, Yang Y, Zhao C, Zhang D, Huang H, Gao J, Li Z, et al. Ascorbic acid enhances Tet-mediated 5-methylcytosine oxidation and promotes DNA demethylation in

mammals. Journal of the American Chemical Society. 2013; 135:10396–10403. [PubMed: 23768208]

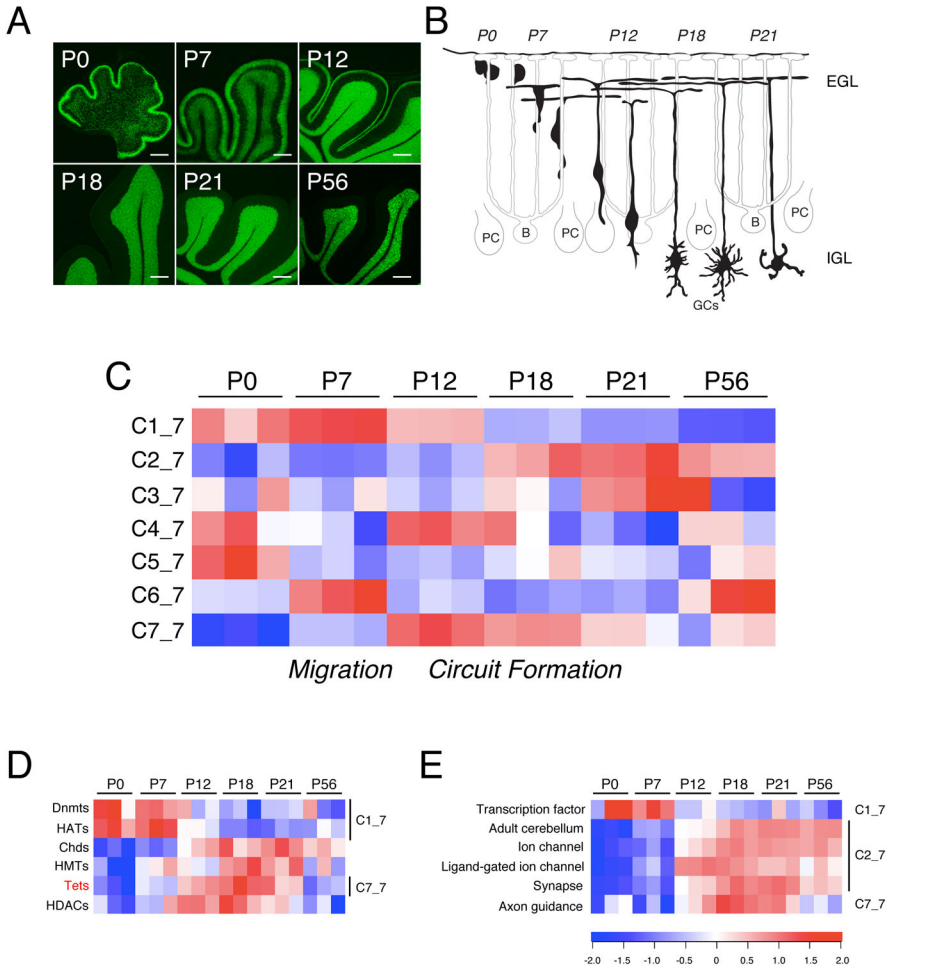


**Figure 1. Metagene Analysis of Cerebellar GC Gene Expression Using TRAP Methodology**

(**A**) NeuroD1-EGFP expression in cerebellar GCs of *Tg(NeuroD1-Egfp-L10a)* TRAP mice at postnatal days 0, 7, 12, 18, 21 and 56 (P0, P7, P12, P18, P21 and P56). Scale bars indicate 80 μm (P56, 125 μm). At P0, most postmitotic, NeuroD1-EGFP+ cells are located in the EGL with only a few positive cells in the IGL. The number of NeuroD1-EGFP+ cells increases between P7 and P12 until P15, when all postmitotic NeuroD1-EGFP+ GCs have migrated into the IGL as shown in (**B**).

(**B**) Progressive developmental stages of cerebellar GCs. By P12, although some GCs are still migrating, the vast majority are post-migratory and are forming synaptic connections. After GCs migrate by the PCs (P18-P21), they become multi-polar, after which they extend dendrites which form connections with ingrowing mossy fiber afferents (P21).

(**C**) Transcriptional profiles of cerebellar GCs at P0, P7, P12, P18, P21 and P56, are decomposed into two matrices and projected into 7 time-dependent metagenes (C1_7-C7_7). “Metagenes” refer to aggregate patterns of gene expression (see text).

(**D**) Expression profiles of epigenetic pathways, including DNA methyltransferases (Dnmts), histone acetyltransferases (HATs), Chromodomain helicase DNA binding proteins (Chds), histone methyltransferases (HMTs), Tet enzymes (Tets) and histone deacetylases (HDACs). The metagene that includes a given set of genes is listed on the right.

(**E**) Expression profiles of gene categories with the most significant difference between immature (P0-P7) and mature cerebellar GCs, including transcription factors and genes highly expressed in adult GCs (Adult cerebellum), ion channels, synaptic genes and axon guidance genes, all of which fall in different metagenes. In the study, expression levels of metagenes, pathways and individual genes are shown as heatmaps which are row normalized ((X - mean(X))/standard_deviation(X)) and cut off at +/- 2. Color bar indicates color intensity for gene expression changes between +/- 2 fold change.
See also Figure S1 and S3.

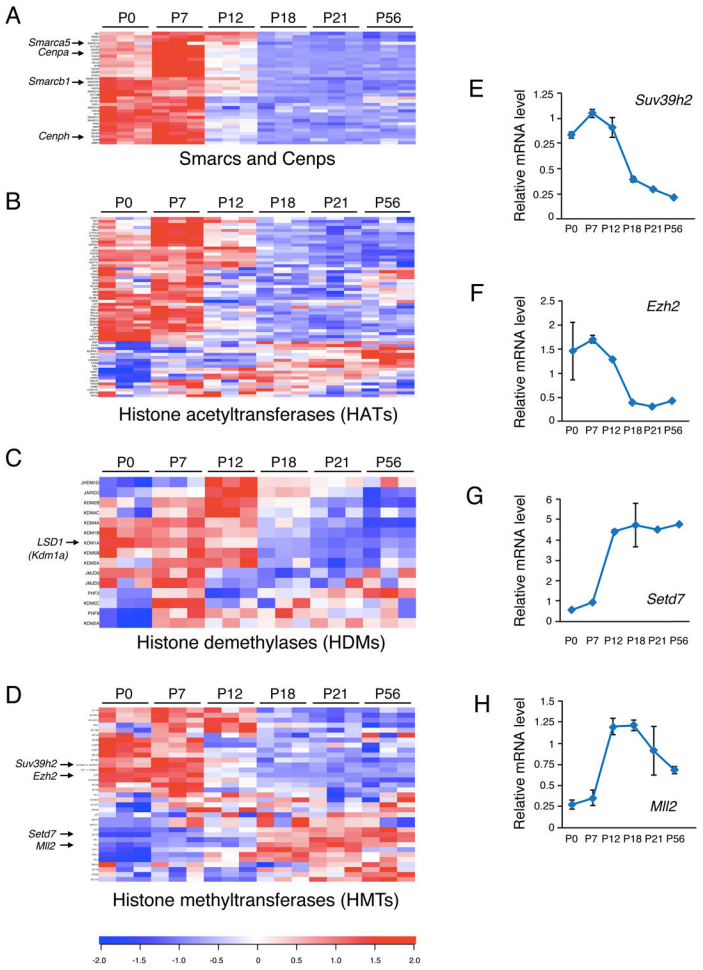


**Figure 2. Sequential Timing of the Expression of Epigenetic Pathway Genes during Cerebellar GC Development**

(**A-D**) Expression patterns of epigenetic genes encoding ATP-dependent chromatin remodeling complexes and centromere proteins (Smarcs and Cenps, C1_7, **A**), HATs (C1_7, **B**), histone demethylases (HDMs, **C**), and HMTs (C1_7 and C2_7, **D**). The heatmaps for different categories of epigenetic genes are organized from **A-D** according to their sequential timing during GC development. Schematic summary of temporal expression of epigenetic genes during cerebellar GC development (P0-P56) is shown in Figure S2D. Genes with known roles in cerebellar GC development (*Smarca5* and *Smarcb1*) and encoding centromere proteins (*Cenpa* and *Cenph*), along with those selected for qRT-PCR analysis (Figure 2A-D), are marked with arrows.

(**E-H**) Expression changes of selected genes were verified by qRT-PCR, including four histone methyltransferases involved in forming the methylation of histone H3 on lysine 4, 9 or 27 (K4, K9 or K27) (*Suv39h2* for H3K9me3, *Ezh2* for H3K27me3, *Setd7* for H3K4me1 and *Mll2* for H3K4me3). In qRT-PCR curve diagrams, Y-axis indicates relative mRNA level normalized to *Beta-2-Microglobulin* and *HPRT1*. Data represent the mean. Error bars indicate SD. Each data point represents nine replicates from three independent biological samples.

See also Figure S2.

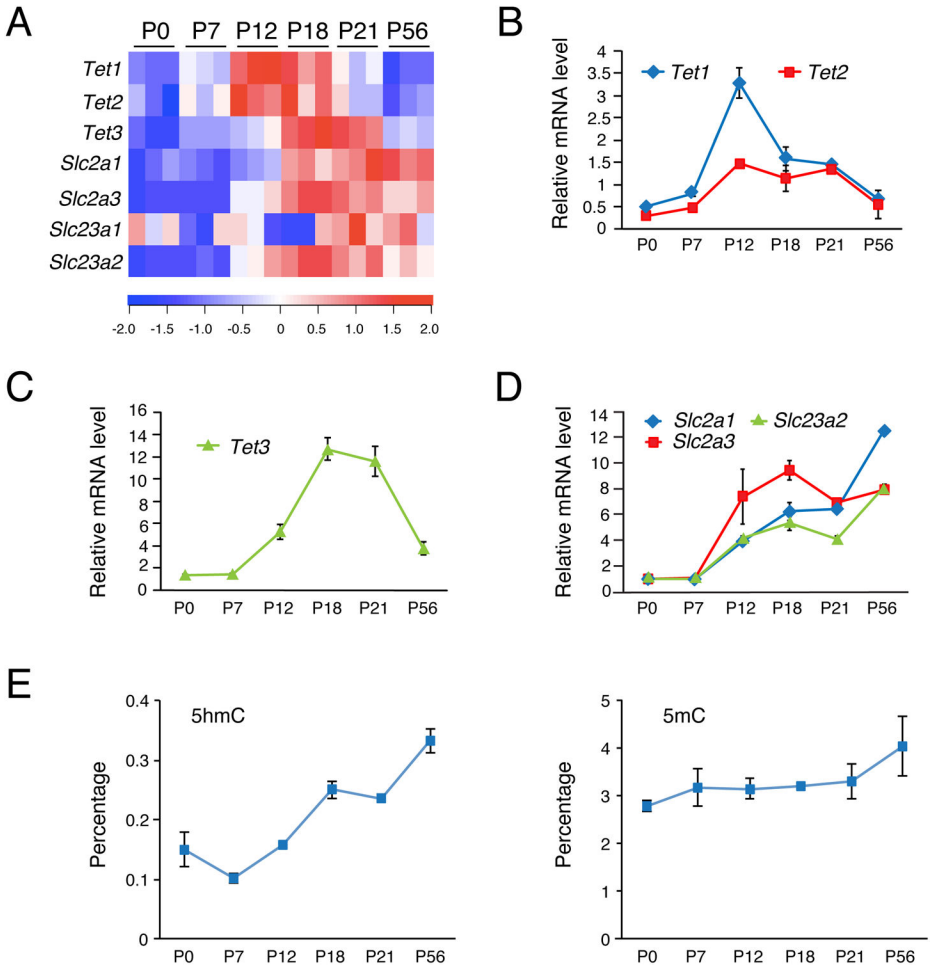


**Figure 3. Increase in Tet Gene Expression and 5hmC Levels During the Period of Circuit Formation in Developing GCs**

(**A**) Expression profiles of Tet genes (*Tet1*, *Tet2* and *Tet3*), which generates 5hmC, and vitamin C transporter genes (*Slc2a1*, *Slc2a3*, *Slc23a1* and *Slc23a2*), which regulate vitamin C levels, in developing cerebellar GCs (P0-P56).

(**B-D**) qRT-PCR analysis of the expression of Tet genes (**B-C**), and vitamin C transporter genes (**D**). In qRT-PCR curve diagrams, Y-axis indicates relative mRNA level with the data normalized to *Beta-2-Microglobulin* and *HPRT1*. Data represent the mean. Error bars indicate SD. Each data point represents nine replicates from three independent biological samples.

(**E**) Percentage of 5hmC and 5mC in genomic DNA purified from mouse cerebellar cortex at different developmental stages (P0, P7, P12, P18, P21 and P56), determined by liquid chromatography-mass spectrometry (LC-MS) analysis. 5mC and 5hmC contents are expressed as the percentage of 5hmC or 5mC in the total pool of cytosine. Data are the mean ± SD from triplicate analyses.

See also Figure S4.

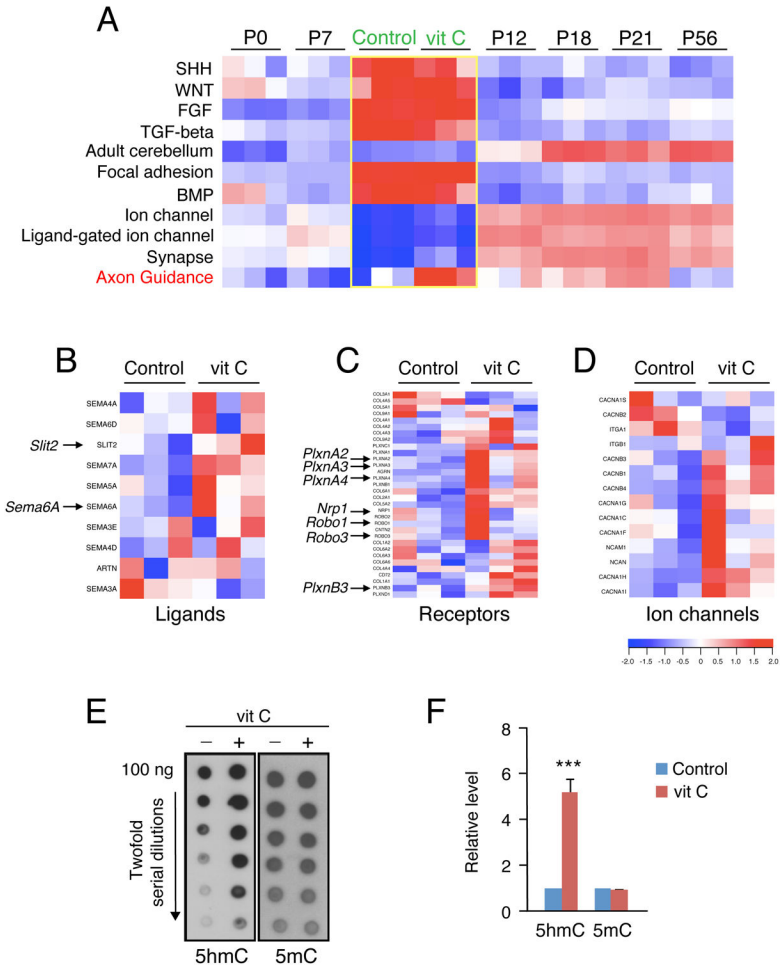


**Figure 4. Vitamin C Treatment Enhances the Expression of Axon Guidance and Ion Channel Genes and 5hmC Levels**

(**A**) Expression profiles of genes involved in signaling pathways (SHH, WNT, FGF, TGF-β and BMP), focal adhesion genes, genes highly expressed in adult GCs (Adult cerebellum), ion channels, synaptic genes and axon guidance genes are shown as a heatmap. A dramatic change in the expression of axon guidance genes (red text) is evident in ES cell-derived GCs treated with vitamin C (vit C, green text and delimited by yellow rectangles).

(**B-D**) Expression profiles of axon guidance ligands (**B**), axon guidance receptors (**C**) and ion channels (**D**) in ES cell-derived GCs treated with vitamin C. Axon guidance genes that function in cerebellar development are marked with arrows.

(**E-F**) Global 5hmC and 5mC levels in ES cell-derived GCs assayed by dot blot analysis (**E**), quantified in (**F**). Data represent the mean, n=3 independent experiments. Error bars indicate SD. ***p<0.001; t-test.

See also Figure S5.

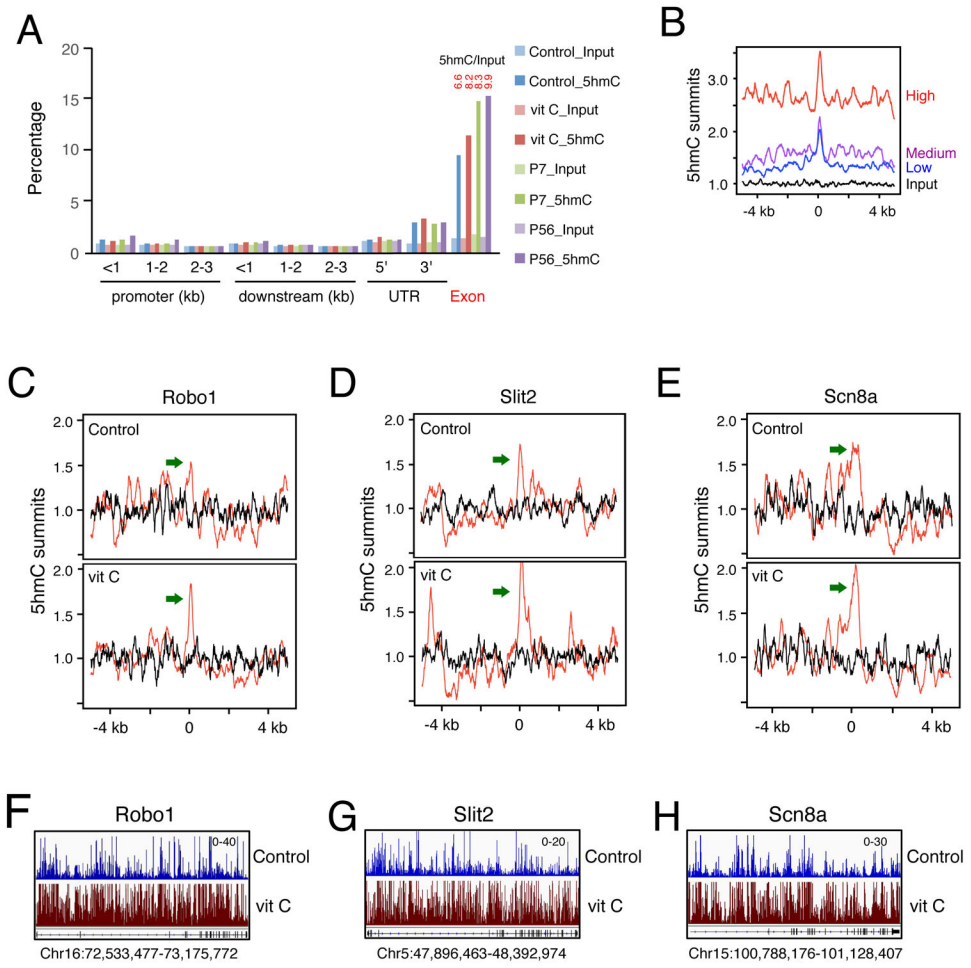


**Figure 5. Increased Expression Levels of Axon Guidance and Ion Channel Genes Correlate with Higher Levels of 5hmC at Exon Start Sites**

(**A**) The relative enrichment of 5hmC (dark color) and input (light color) at genomic elements in ES cell-derived GCs without treatment (Control, blue) and with vitamin C treatment (vit C, red), and cerebellar GCs at P7 (P7, green) and P56 (P56, purple). In the diagram, Y-axis indicates the percentage of 5hmC peaks distributed into each genomic element over all called peaks in each cell type (Figure S6A). The enrichment ratio (5hmC/Input) is highest for exons (red text) and is indicated at the top of the exon columns.

(**B**) Highest 5hmC levels map to the exon start sites of the most highly expressed genes. Aligned profiles of 5hmC enrichment over exons are categorized by gene expression levels (High, Medium, Low and Input) (see Supplemental Experimental Procedures). “Exon start site” refers to all exons. The X axis is the distance from the exon start site, which is set as “0” in kilobases (kb).

(**C-E**) Increased 5hmC levels in *Robo1* and *Slit2*, a representative axon guidance receptor and ligand gene, respectively, and *Scn8a*, an ion channel important for cerebellar development, in control and vitamin C treated ES cell-derived GCs. The 5hmC line plots (**C-E**, marked in red) are indicated with normalized average 5hmC summits (Y axis). The X axis is the distance from the exon start site, which is set as “0” in kilobases (kb). The maximal 5hmC level is seen at exon start sites (green arrow). Input line plots are marked in

black at the bottom. The increase in *Robo1* and *Slit2* expression in ES cell-derived GCs treated with vitamin C is seen in Figure 4B-C.

(**F-H**) Intragenic 5hmC peaks in *Robo1*, *Slit2* and *Scn8a* in ES cell-derived GCs without (control, blue) and with vitamin C treatment (vit C, red), are shown using Integrative Genomics Viewer (IGV). The last row in black represents the gene bodies located in this particular region of the genome. (The scale of the peaks is indicated in the upper right side of the control panel.)

See also Figure S6 and S7.

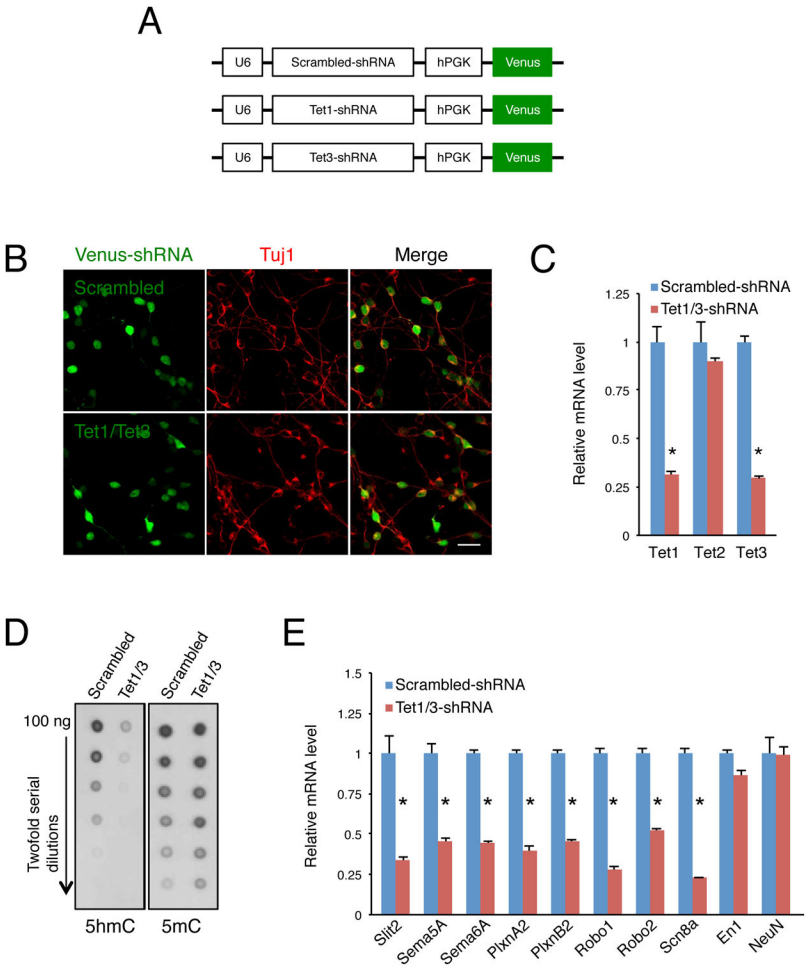


**Figure 6. Tet RNAi Knockdown Decreases 5hmC Levels and Down-regulates the Expression of Axon Guidance and Ion Channel Genes**

(**A**) Schematic diagrams of Venus-shRNA constructs. The human U6 promoter (U6) drives RNA Polymerase III transcription for generation of shRNA transcripts, and the human phosphoglycerate kinase promoter (hPGK) drives expression of Venus.

(**B**) Purified P7 cerebellar GCs transfected with *Tet1/3* shRNA plasmids that co-express the fluorophore Venus and stained for Venus and Tuj1 (red) are viable after 3DIV. Scale bar: 25 μm.

(**C** and **E**) The expression levels of selected genes in purified P7 cerebellar GCs when *Tet1* and *Tet3* were knocked down were determined by qRT-PCR. Purified GCs at P7 were infected with lentiviral particles of shRNA plasmids targeting *Tet1* or *Tet3* and co-expressing the fluorophore Venus. Scrambled shRNA was used as a control and the expression level of selected genes in the control cells was set as 1. In the qRT-PCR histogram, Y-axis indicates relative mRNA level normalized to *Beta-2-Microglobulin* and *HPRT1*. Data represent mean. Error bars indicate SD. Each data point represents nine technical replicates from three independent biological samples. *p<0.05; t-test.

(**D**) RNAi knockdown of *Tet1/3* in purified P7 cerebellar GCs. By dot blot analysis, 5hmC levels decrease and 5mC levels increase slightly.

See also Figure S7.

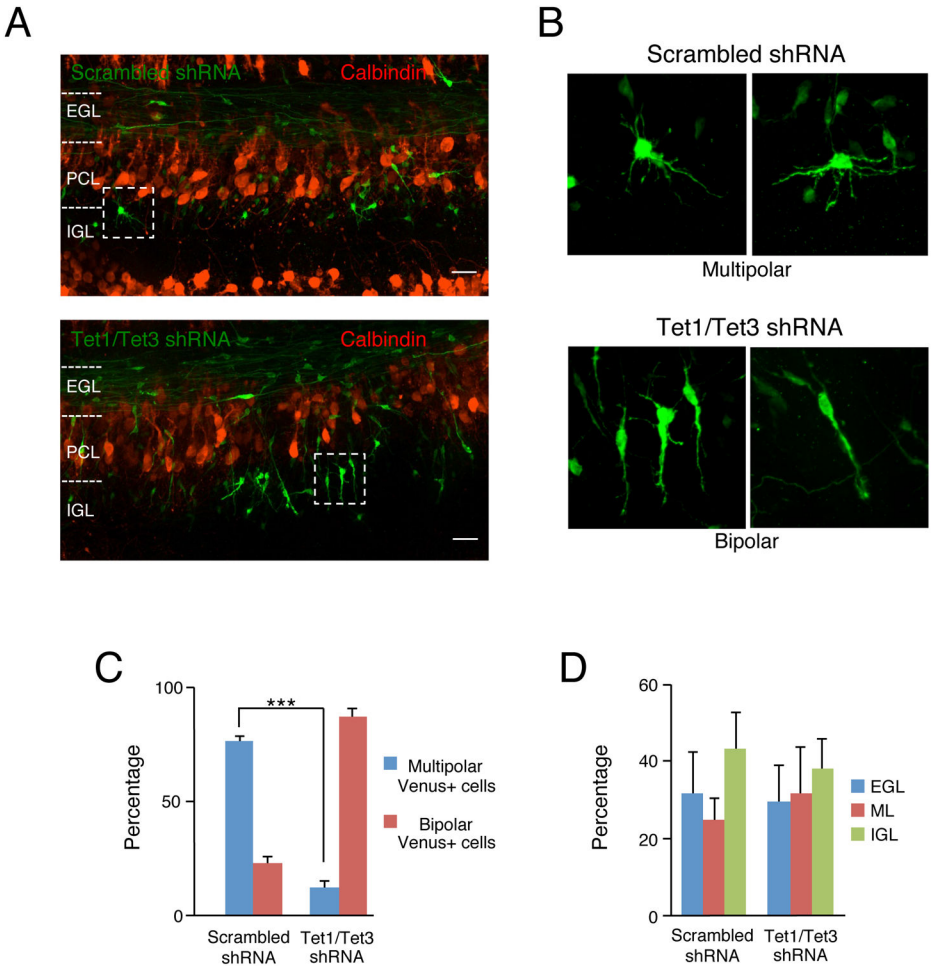


**Figure 7. Tet Knockdown Impairs Dendritic Arborization of Cerebellar GCs**

(**A**) Coronal slices of P7 mouse cerebella electroporated with equal amounts of *Tet1* and *Tet3* shRNA plasmids or scrambled control shRNA plasmid that co-express the fluorophore Venus were cultured for 3 days and immunostained for Venus (green) to visualize the transfected GCs and for Calbindin (red) to visualize PCs. Major developmental layers are indicated. EGL, external granule layer; PCL, Purkinje cell layer; IGL, internal granular layer. Scale bar: 1 mm.

(**B**) Higher magnification images showing dendritic growth of labeled GCs in cerebellar slices transfected with the scrambled or Tet shRNA constructs. Multipolar GCs extending dendrites are seen throughout the IGL deep to the PCs.

(**C-D**) Tet knockdown impairs dendritic arborization of cerebellar GCs without affecting GC migration. Quantification of the effect of *Tet1* and *Tet3* gene knockdown on dendritic growth (**C**) and GC migration (**D**) observed at 3 DIV. Data depicts average percentage (Error bars, SD) from four different cultures (approximately 30-40 cells counted in each selected region) for each condition. (***$p < 0.001$; t-test). See Figure 1B for a schema of GC developmental stages.

See also Figure S7.